RIT
College of Science
School of Chemistry and Materials Science

Crystallized DNA G-Quadruplex Structure Bound to an Iridium Complex Ligand

Authors: Lee Schoneman, Adam Robinson, Rachel Horowitz, Dr. Carly Reed, Dr. Michael Gleghorn

Background

G-quadruplexes form structures ranging from one nucleic acid strand to up to four strands and, depending on the direction of which the DNA strands orient, can be classified as either parallel or anti-parallel. To be classified as a parallel G-quadruplex, all strands in the structure must be parallel; if one or more strands are in an anti-parallel conformation, the entire structure is deemed anti-parallel. The looping of DNA is only observed in unimolecular and bimolecular structures, as tetramolecular structures form from four separate nucleic acids and thus do not need to turn outside the structure to change direction.

Once a G-quadruplex has formed, ligands may bind to various areas on the structure. If the top of the quadruplex is available, for example, planar ligands, such as the iridium (III) complex, tend to bind in that location, resulting in the iridium complex exhibiting enhanced fluorescence. However, in the presence of double and single stranded DNA, the complex experiences no change in fluorescence. It is suggested that the ligand interacts with the loops of DNA formed when the strands of the quadruplex changes direction as well as the G-quartet, providing the ability to locate a G-quadruplex that is interspersed with double-stranded DNA, as would be the case *in-vivo*.

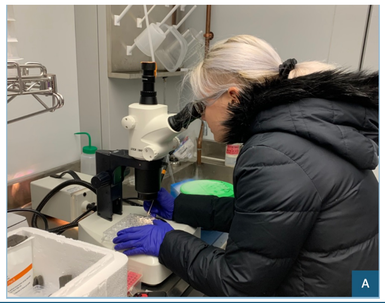

Methodology

Method 1: Ligand Soaking

To screen for optimal conditions to grow native G-quadruplex crystals using the oligonucleotide sequence 5'-TGGGGT-3', crystal conditions known to allow G-quadruplex formation were utilized (Clark et al, PDB ID: 100K). Conditions contained varying concentrations of sodium chloride [110 – 245 mM], calcium chloride [6 – 24 mM], and 2,4-methylpentanediol (MPD) [2 – 15% v/v], in addition to 20 mM sodium cacodylate HCl buffer (6.5 pH) and 6 mM spermine tetrahydrochloride (Table A). In each well, 1 µL of the respective crystal condition was added to 1 µL of annealed DNA solution. In addition to differences in crystal conditions, DNA concentration of the annealing solution varied between trays to reduce the formation of microcrystals, ranging from 0.5625 mM to 4.5 mM. The crystal tray was stored at 4 degrees Celsius. Observations on crystal growth were recorded on the fourth day and sixth day after tray creation, with further observations recorded weekly as necessary. For crystal conditions that consistently produced larger and less nucleated crystals (refer to starred well names in Table A), the crystals were soaked with 4 µL of a saturated solution of our cyclometalated iridium complex (RHH111319 or "Ir pizp") (Figure C) in 100% MPD.

Method 2: Cocrystallization

To create the cocrystallization conditions, Ir pizp was dissolved in 100% MPD prior to creating the crystal condition solutions. Concentrations of reagents mirrored those found in Table A, and the procedure for creating the crystal tray followed the one used for the ligand soaking. Data on these trays has not been collected.

Data Collection

All crystal trays were transported to Hauptman-Woodward Medical Research Institute for collection. Samples were then shipped to Brookhaven National Laboratory for diffraction. X-ray diffraction experiments were conducted at Brookhaven National Laboratory using the FMX beam at the National Synchrotron Light Source II (NSLS II). Using PHENIX and Coot, the electron density maps for both native and soaked crystals were analyzed and mapped.

Abstract

Oncogenes contain many tumor survival pathways that, when overexpressed, can result in carcinogenesis. One method that may hinder oncogene production is G-quadruplex formation in the promoter region of the gene. In a G-quadruplex, four guanine bases bind to one another instead of traditional base pairing. Due to the size and complexity of the quadruplex, RNA polymerase cannot advance, and transcription is halted. The presence of G-quadruplexes can be confirmed using an iridium complex as a ligand, due to its increased luminescence once bound to a quadruplex. To determine the binding position of such a ligand, we grew crystals containing an oligonucleotide sequence known to form G-quadruplexes before introducing the ligand to the crystal. Crystals were analyzed using X-ray diffraction and the electron densities were modeled to determine the structure. While structure determination is still in progress, understanding these interactions will provide insight into how to locate G-quadruplexes in vivo.

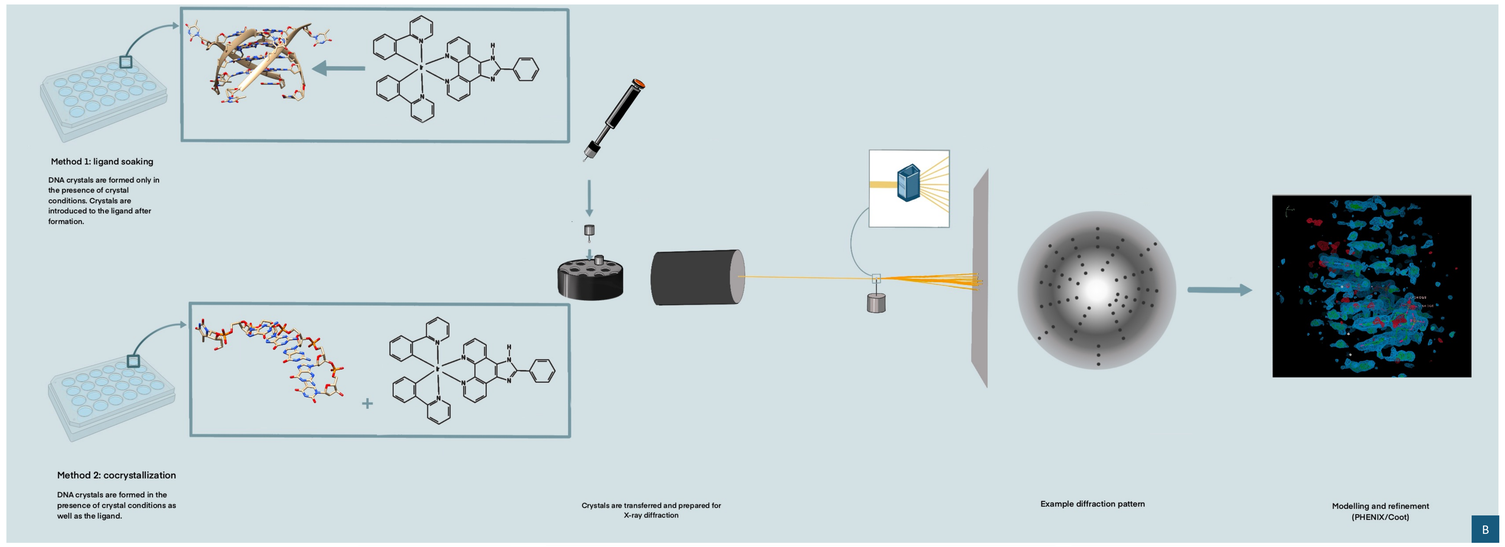

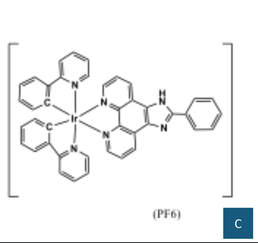

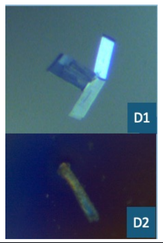

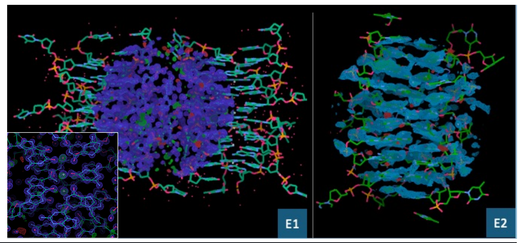

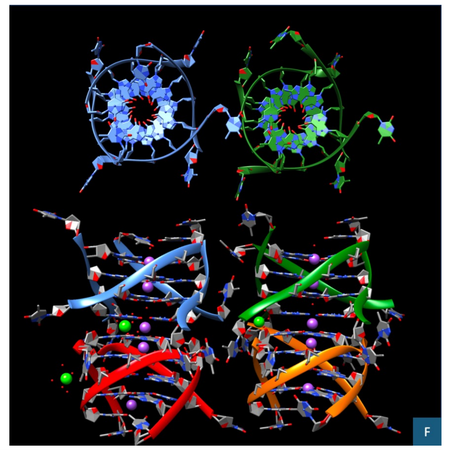

Salt Concentration	*Well 1*	*Well 2*	*Well 3*	*Well 4*	*Well 5*	*Well 6*
Row A	A1	A2	A3	A4	A5	A6
110 mM NaCl, 6mM $CaCl_2$	110 mM NaCl, 6 mM $CaCl_2$, 2% MPD v/v	110 mM NaCl, 6 mM $CaCl_2$, 4.6% MPD v/v	110 mM NaCl, 6 mM $CaCl_2$, 7.2% MPD v/v	110 mM NaCl, 6 mM $CaCl_2$, 9.8% MPD v/v	110 mM NaCl, 6 mM $CaCl_2$, 12.4% MPD v/v	110 mM NaCl, 6 mM $CaCl_2$, 15% MPD v/v
Row B	B1	B2	B3	B4	B5	B6
155 mM NaCl, 12 mM $CaCl_2$	155 mM NaCl, 12 mM $CaCl_2$, 2% MPD v/v	155 mM NaCl, 12 mM $CaCl_2$, 4.6% MPD v/v	155 mM NaCl, 12 mM $CaCl_2$, 7.2% MPD v/v	155 mM NaCl, 12 mM $CaCl_2$, 9.8% MPD v/v	155 mM NaCl, 12 mM $CaCl_2$, 12.4% MPD v/v	155 mM NaCl, 12 mM $CaCl_2$, 15% MPD v/v
Row C	C1	C2	C3*	C4	C5*	C6*
200 mM NaCl, 18 mM $CaCl_2$	200 mM NaCl, 18 mM $CaCl_2$, 2% MPD v/v	200 mM NaCl, 18 mM $CaCl_2$, 4.6% MPD v/v	200 mM NaCl, 18 mM $CaCl_2$, 7.2% MPD v/v	200 mM NaCl, 18 mM $CaCl_2$, 9.8% MPD v/v	200 mM NaCl, 18 mM $CaCl_2$, 12.4% MPD v/v	200 mM NaCl, 18 mM $CaCl_2$, 15% MPD v/v
Row D	D1	D2	D3*	D4	D5	D6
245 mM NaCl, 24 mM $CaCl_2$	245 mM NaCl, 24 mM $CaCl_2$, 2% MPD v/v	245 mM NaCl, 24 mM $CaCl_2$, 4.6% MPD v/v	245 mM NaCl, 24 mM $CaCl_2$, 7.2% MPD v/v	245 mM NaCl, 24 mM $CaCl_2$, 9.8% MPD v/v	245 mM NaCl, 24 mM $CaCl_2$, 12.4% MPD v/v	245 mM NaCl, 24 mM $CaCl_2$, 15% MPD v/v
MPD (percent volume per volume)	2%	4.60%	7.20%	9.80%	12.40%	15%

Image Descriptions

Figure A (leftmost image): *Crystal collection at HWI.* **Figure B** (topmost image): *Graphical demonstration of the procedure used to grow, collect, and analyze the contents of our crystals.* **Figure C** (second row, first image): *Our collaborator's ligand of interest – a cyclometallated iridium (III) complex, which luminesces when bound with G-quadruplexes.* **Figure D** (second row, second image)*: An example of the crystals containing G4 DNA. These crystals in particular were involved with the ligand soaking procedure (D1) and the cocrystalization procedure (D2).* **Figure E** (second row, third image): *Refined electron density maps and models for G-quadruplex crystal samples including results from one native crystal (E1) as well as results from one ligand-soaked crystal outlier (E2).* **Figure F** (rightmost image): *Refined model showcasing four quadruplexes; two of which are stacked against each other.* **Table A** (bottom row) *Documentation of all crystal conditions used in the screening process, categorized by the rows and columns of the tray.*

Results

Crystal Screening

The majority of crystal conditions produced crystals, but few were able to produce crystals of considerable size. Wells rarely produced precipitate, but, when present, were typically accompanied by G4 crystals.

Diffraction Data

Overall, samples produced data with relatively high resolution, averaging at 0.964 Å for native G4 crystals and 1.239 Å for soaked G4 crystals, with samples having a highest resolution of 0.92 Å and 0.97 Å respectively. Across all samples, crystals contained the same space group (P1), and most crystals had similar unit cell dimensions (a = 28.3 ± 0.1, b = 34.85 ± 0.05, and c = 56.25 ± 0.15, with α, β, and γ equaling 74.3 ± 0.1, 77.75 ± 0.15, and 89.75 ± 0.15). One ligand-soaked crystal sample had slightly smaller unit cell dimensions however, containing lengths of 27.4, 27.8, and 35.0 Å and angles equaling 89.1, 75.5, and 79.6 Å.

Model Building and Refinement

Using a G-quadruplex as a model (PDB ID 352D), the electron density map was refined to an R-free value of 0.2089 for the native crystals (Figure E1). For the ligand-soaked samples, R-free values averaged at 0.2695, not including two outliers that contained R-free values of 0.548 and 0.5542, which were from the sample that had decreased unit cell dimensions (Figure E2).

Discussion

Crystal Screening

Due to overnucleation, the DNA annealing solution (originally containing 4.5 mM G4 DNA) was diluted with double distilled water multiple times, with the lowest concentration of G4 DNA tested (0.5625 mM) yielding the largest crystals.

Crystal conditions containing greater percentages of MPD (greater than or equal to 7.2 percent volume per volume) as well as greater salt concentrations (mostly consisting of the lower two rows of crystal screening trays) tended to yield larger, less nucleated crystals in native conditions (Figure D1). Although these crystals were larger, they were still on the smaller side of the sizes needed to undergo X-ray diffraction. For crystals that underwent soaking, the crystals tended to crack after being introduced to the ligand, which risked the integrity of the crystal and made them more difficult to collect, which may have impacted diffraction data.

Although cocrystallization of the iridium complex with the DNA is still in progress, crystal formation appears to take longer than native G4 crystals when comparing crystal growth by observations recorded after the same duration since tray creation (Figure D2).

Diffraction Data

The resolution of the native crystals is comparable to the resolution of previous models, if not slightly better. It may be worthwhile to see if the native model can be improved, as a few terminal residues appear to have little to no corresponding electron density.

Model Building and Refinement

Despite the presence of a weak anomalous signal during data collection which could have been attributed to the iridium complex, no unmodelled areas of electron density were able to be assigned to the compound, suggesting that the compound was unable to bind to the quadruplex.

In regard to the sample with smaller unit cell dimensions, it does not appear that there are any major differences between it and other soaked crystals, other than the fact that only two G-quaduplexes were able to fit in the unit cell rather than the accepted amount of four (Figure F).

Sources

Burge, S.; Parkinson, G. N.; Hazel, P.; Todd, A. K.; Neidle, S. Quadruplex DNA: sequence, topology and structure. *Nucleic Acids Res* 2006, *34* (19), 5402-5415. DOI: 10.1093/nar/gkl655.

Castor, Katherine J., et al. "Cyclometalated Iridium(Iii) Imidazole Phenanthroline Complexes as Luminescent and Electrochemiluminescent G-Quadruplex DNA Binders." Inorganic Chemistry, vol. 54, no. 14, 30 June 2015, pp. 6958–6967., https://doi.org/10.1021/acs.inorgchem.5b00921.

Clark, George R., et al. "Structure of the First Parallel DNA Quadruplex-Drug Complex." Journal of the American Chemical Society, vol. 125, no. 14, 15 Mar. 2003, pp. 4066–4067., https://doi.org/10.1021/ja0297988.

Lin, S.; Wang, W.; Hu, C.; Yang, G.; Ko, C.-N.; Ren, K.; Leung, C.-H.; Ma, D.-L. The application of a G-quadruplex based assay with an iridium(iii) complex to arsenic ion detection and its utilization in a microfluidic chip. *Journal of Materials Chemistry B* **2017**, *5* (3), 479-484, 10.1039/C6TB02656G. DOI: 10.1039/C6TB02656G.

Phillips, Kathryn, et al. "The crystal structure of a parallel-stranded guanine tetraplex at 0.95Å resolution" Journal of Molecular Biology, Volume 273, Issue 1, 1997, Pages 171-182, https://doi.org/10.1006/jmbi.1997.1292.

Acknowledgements

Dr. Michael L. Gleghorn and the Gleghorn Research Lab at RIT, Alexei Soares, RIT College of Science, RIT Emerson Summer Undergraduate Research Fellowships (SURF), Hauptman-Woodward Medical Research Institute, Brookhaven National Laboratory